A Concurrent Patient-specific Musculoskeletal and Finite Element Modeling Framework for Predicting in Vivo Kinematics and Contact Mechanics of Total Knee Replacement

[1]Liming Shu, [1]Naohiko Sugita, [2]Prabhav Saraswat, [2]Jiang Yao, [1]Reina Yoshizaki, [1]Ko Yamamoto, [1]Mamoru Mitsuishi

1 Department of Mechanical Engineering, School of Engineering, University of Tokyo, Tokyo, Japan

2 Dassault Systemes Simulia Corp., Providence- RI, USA

***Abstract**: Understanding the kinematic and contact mechanics for in vivo specific patient has dictated the success of current total knee replacement (TKR) prostheses. In this paper, an in vivo predicting method to analyze kinematic and contact mechanics within specific TKR knee joint has been proposed and experimentally verified based on concurrent dynamic finite element model (FEM) and patient-specific musculoskeletal (MS) technology, which was achieved by the commercial software Abaqus and Isight from Dassault Systemes. The hybrid MS model was built mainly including three parts, namely cadaver-based MS model, subknee model and deformable FE prosthesis model, based on CT images. Nonlinear programming carried out by quadratic lagrangian (NLPQL) method was utilized to scale and position the hybrid MS model, on the basis of the patient-specific parameters of two patients implanted with an instrumented TKR from the fourth and sixth "grand challenge competition to predict in vivo knee loads" database. In order to reproduce the lower limb kinematic, the inverse kinematic has been implemented based on multiple marker points distributed coupling method from Abaqus. The predicted results show a good agreement (RMSE=3.75°, R2= 0.985) with fluoroscopic experimental results. For the TKR knee joint, where 6 degree of freedom was set on tibio-femoral joint, an advanced concurrent inverse dynamics and quasi-static FE method has been created to solve the joint kinematic and contact mechanics in Abaqus by using Python script based on ground reaction force, ligament force and muscle force. The modeling framework has potential applications in aiding the subjective surgical planning in orthopedics procedures and providing a comprehensive tool for customer-made-prosthesis design.*

***Keywords**: Biomedics, Coupled Analysis, Experimental Verification, Multi-Body Dynamics, Total knee replacement, musculoskeletal model*

1. Introduction

Joint replacement surgery is an effective procedure to relieve pain, correct leg deformity, and help patents resume normal daily activities. Knee replacement surgery was first performed in 1968. Since then, improvements in surgical materials and techniques have greatly increased its effectiveness. However, the knee implant geometric structure is highly standardized and surgical plan is mostly subjective, causing surgical outcomes to be highly variable for different patients and surgeons. What's more, the biomechanical properties around the knee joint are controlled by complex interactions among the forces of muscles, ligaments, bone geometry, a variety of other soft tissues, and the surrounding environment. An in vivo measurement is very difficult to be produced without the invasive procedures. In order to solve the above problems, a wide range of experimental and computational methods have been designed and used to analyze preclinical TKR performance. The musculoskeletal model, which encompasses a skeleton consisting of rigid body segments (bones) connected by joints and muscles, has been believed as a potential method to consider the individual characteristics of patients on biomechanical analysis and simulation. Marco et al. [1,2] developed a subject-specific MS framework for TKR based on concurrent of inverse dynamics and force-dependent kinematics methods to predict in vivo knee loads and knee joint kinematics, which were verified by the experimental data from fifth "grand challenge competition". Thelen et al [3] presented a co-simulation framework of body-level MS dynamics and knee mechanics on gait. Their method was developed based on a computed muscle control algorithm and forward dynamics, which was able to predict muscle activations, knee kinematics and tibiofemoral contact force. However, the prosthesis component in the MS model was considered as a rigid body in order to simplify the calculation, which cannot meet the accuracy requirements of surgery. Moreover, the outputs of the MS model, namely contact force, torque and pressure, cannot be used to intuitively evaluate the effect of TKR. The optimal stress distribution and contact mechanics within the prosthetic components are two of main design objectives to increase the service life of TKR, which can be calculated by means of the nonlinear FE method. FEM simulations have already been a standard developed tool in mechanical or materials engineering. In biomechanics, they have been used to carry out various analyses of soft tissues, such as simulations of mechanical behavior of arteries [4] and intervertebral discs [5], analyses of joints, implants and bones, which are, in orthopedic, often focused on bone tissue behavior after an arthroplasty [6–8]. Sathasivam and Walker [9] presented an implicit FE analysis driven by kinematic inputs from ISO standard to predict stresses of tibia insert in a prosthesis system during gait. Whereas the kinematic inputs are varied with patients.

To the best of the authors' knowledge, this is the first attempt to integrate FE and MS model for investigating the real time kinematics and contact mechanics of a prosthetic leg for a specific patient. With the preceding discussion in mind, this paper aims to develop a high fidelity subject-specific MS-FE model with lower extremity based on subject-specific computed tomography images, motion capture data, and force plate data. The model is capable of predicting in vivo stress distribution and contact mechanics allowing individualized treatment plans and individualized prosthesis designs. For enhancing the accuracy of the simulation, an advanced concurrent inverse dynamics and quasi-static FE method has been created to solve the joint kinematic and contact mechanics in Abaqus by Python script based on ground reaction force, ligament force and muscle force. The framework is verified and evaluated by an instrumented TKR patient from the fourth and sixth "grand challenge competition to predict in vivo knee loads" database via a human right lower limb model.

2. Methods and materials

2.1 Subject data

The patient data used in the research were obtained from the fourth and sixth grand challenge dataset from the grand challenge competition to predict in vivo knee loads [10]. The experimental data were obtained from two male subjects (JW: age—83, height—166 cm, and body weight—64.6kg; DM: age—83, height—172 cm, and body weight—70kg), who took a posterior cruciate-retaining (PCR) total knee replacement (TKR) on their right knees. Two kinds of different implants have been used on the subjects. The implant on the subject JW, a generation I tray design (eTibia), was equipped with four piezoelectric force-measuring sensor that can be used to measure the axial force, center of pressure and AP/ML Moments [11]. An advanced generation II tray design equipped with a telemetric force-measuring sensor was used on the subject DM. The 3 DOFs force and 3 DOFs moment can be in vivo measured during the movement of subjects. Systematic experimental data were provided in dataset, which included eTibia loads, trajectories of motion capture markers, force plate data, EMG for a series of gait trials, joint calibration trials and fluoroscopy trials, and pre- and postoperative CT data. The 3D geometries of the prostheses and bone were provided in geometric stereo lithography (STL) format.

2.2 Subject-specific MS-FE model

The subject-specific MS-FE model mainly includes the MS base model, subknee model, and prosthesis model, which combines the MS analysis with the FE analysis. The detailed workflow of the simulator is shown in Fig.1. All the models were developed in Abaqus CAE.

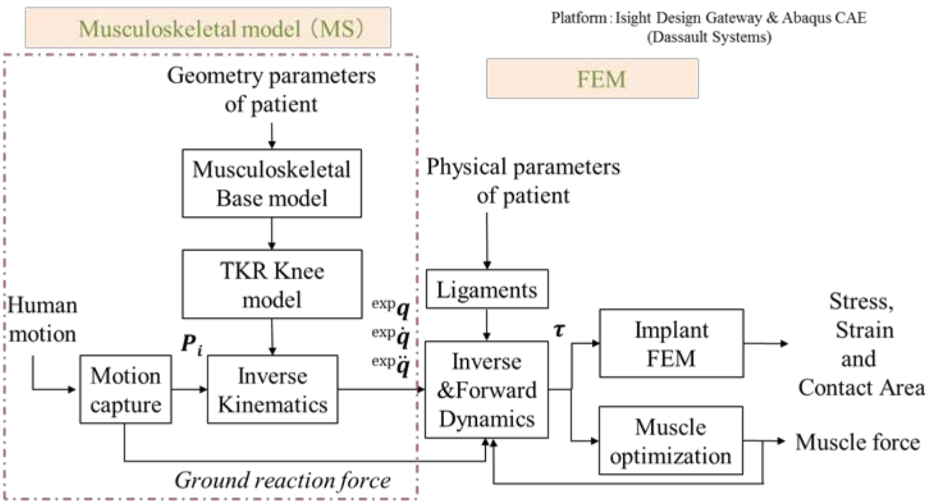

Figure.1. Workflow of simulator

2.2.1 MS base model

A cadaver-based MS model was developed by commercial software (Abaqus and Isight) provided by Dassault Systemes Simulia Corp. [12], as shown in Fig.2 (a). The center of mass (COM), muscle insertion coordinates and muscle parameters were taken from Delp *et al.* [13]. The joint between each segment was defined based on anatomical kinetic properties. Forty-three muscle–tendon (MT) units were represented with three component Hill-type one-dimensional axial connector elements spanning from origin to insertion through via-points and wrapping over analytical surfaces fitted to the bone geometries in Abaqus. All the bone segments were set as a display body. The reference points of muscle and COM on each segment were set as a rigid body. The marker point system was set based on coordinates from the Subject-Specific OpenSim Model from the fourth grand challenge competition.

2.2.2 Subknee model

In order to specify the geometric detail of knee joint for each patient, a 3D subknee model was developed based on CT scan from the dataset, as shown in Fig.2 (b). The STL format model was imported into Hypermesh^{TM} to create the quadrilateral elements for FE analysis. Ligaments around the knee joint were modeled as one-dimensional axial connecters with no compressive stiffness and nonlinear tensile stiffness based on experimental tensile testing on lateral collateral ligament (LCL), medial collateral ligament (MCL) and posterior cruciate ligament (PCL), scaled by dimensional differences in cross sectional area and length between the experimental sample and this subject's geometry [14-16]. The anterior cruciate ligament (ACL) was not modeled in the simulation, since it was sacrificed during the surgery. The tangent constraint of MCL on knee joint was set by nodes to surface contact. Since attachment sites could not be determined from the dataset, they were estimated according to model from OpenKnee [17].

2.2.3 Prosthesis model

Implant components used in the framework were reversely engineered from defeatured point files sampled from the original CAD models, where disfeaturing was performed only outside of the contact surfaces, as shown in fig.2(c). The Hypermesh^{TM} has been used to remesh the STL format triangular elements into the tetrahedral elements. The material of tibial insert component was UHMWPE defined as elastic-plastic material, while that of femoral and tibial tray components was CoCrMo. The material properties are listed in Table.1. All of the components were meshed by C3D10 element. The average element size of femoral component, tibial insert component and tibial tray components were set as 2.2mm, 1.8mm and 2.2mm, respectively. The total number of prosthesis elements after meshed are 191,994.

In order to obtain a high accurate joint centers and axes, we performed analytical surface fits on the postoperative bones, as shown in Fig. 2(d). 3D subknee was coupled to preoperative MS bone model based on iterative closest point algorithm [18]. Some manual adjustments also were implemented in this part.

Table.1 Material property of prosthesis components

Material	**Density (kg/m^3)**	**Elastic Modulus (GPa)**	**Poisson's ratio**
CoCrMo	7610	217	0.3
UHMWPE`	932e	1	0.45

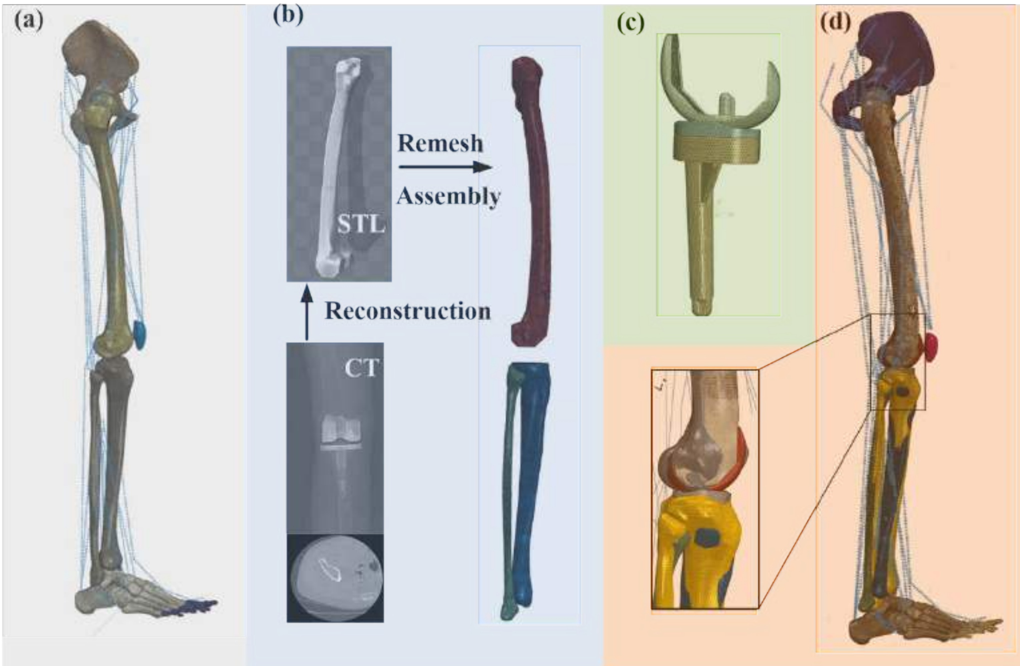

Figure.2. (a) MS model developed in Abaqus, (b) subknee model, (c) prosthesis components, (d) TKR model after prosthesis position and subknee registration

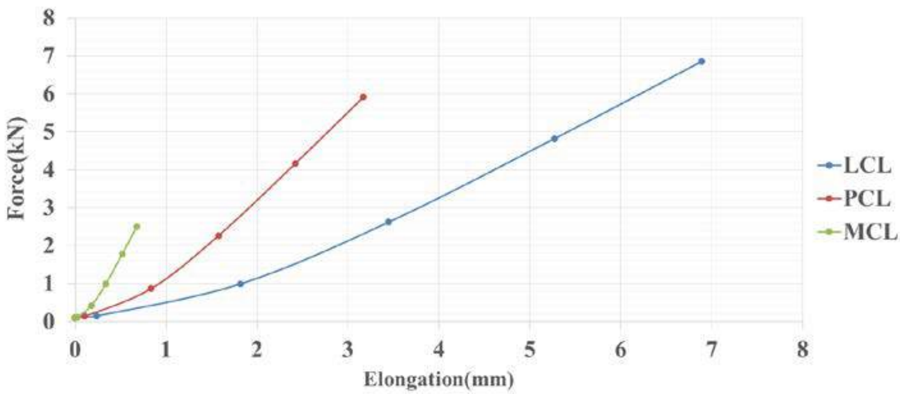

Figure.3. The mechanical property of ligaments around knee joint

2.3 Scaling & Positioning

Patient-specific musculoskeletal models were developed by scaling and positioning the base model through using the average static posture frame of the marker position in motion capture data from the dataset. The marker was set based on the description of motion capture marker placement for the fourth grand challenge competition. The Isight^{TM} optimization module (Nonlinear programming by quadratic lagrangian (NLPQL)) [19] was utilized to compute the scaling and transformation matrices, as shown in Figure 4. The objective function was to minimize the least square error of marker coordinates while ball hinge constraints were applied on hip, knee and ankle joints. The cameras record the centroid of spherical marker on skin rather than anatomical location on the bone. Hence, the marker offset optimization varied with 5-15 mm bound also was implemented in the optimization. The schematics of model scaling is shown in Figure 5. The muscle attachment points and COM of each segment were scaled and positioned with the segment.

2.4 Inverse kinematics

After the model scaling, an inverse kinematics method was used to track the marker trajectories during a normal gait from the grand challenge competition dataset (jw_ngait_og1.c3d) providing the time history of the following lower limb kinematics. Motion of 3-4 markers on each leg segment was reduced to 6 DOFs (3 translations & 3 rotations) for each rigid segment in Abaqus^{TM}. The step was carried out by a combination between shell elements and distributed coupling feature to filter out the skin motion artifact from the motion data. Amplitude file generated was used to drive the COM of each segment of MS model. The patella-femur (PF) joint movement was controlled by the relationship between femur-tibia (FT) flexion and PF movement [20]. The PF joint was further constrained by enforcing a fixed-length patellar ligament.

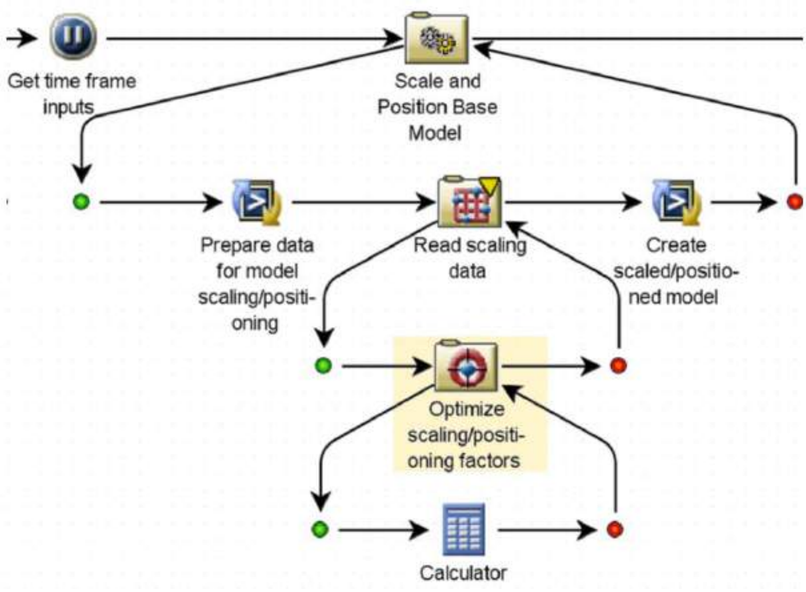

Figure.4. Current Implementation of Patient-specific musculoskeletal model （Isight Optimization）

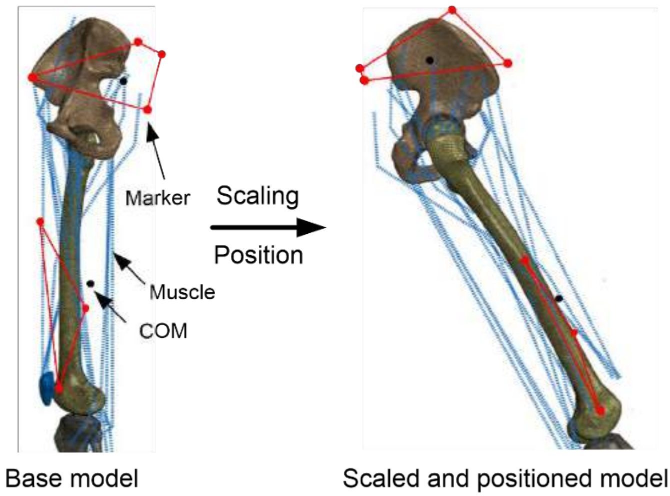

Figure.5. Schematics of base model and scaled model

2.5 Inverse&Forward dynamics

The ground reaction force (GRF) was achieved from force plate. Amplitude files on COM of hind foot were generated and imported into Abaqus^{TM} from GRF (Fx, Fy, Fz, Mx, My, Mz), as

$$F_{\mathrm{COM}} = F_{\mathrm{COP}} \tag{1}$$

$$M_{\mathrm{COM}} = r \times F_{\mathrm{COP}} + T_z \tag{2}$$

$$r = COP - COM \tag{3}$$

Where, F_{COM} and F_{COP} are the GRF on the *COM* and contact point of force plate, respectively; M_{COM} is the moment on *COM* from ground reaction; T_{z} is the moment on *COP* from ground reaction; r is the distance from *COP* to *COM*. The history outputs of joint angles and GRF were input to the inverse dynamic analysis in MS analysis. For reproducing the real kinematics of knee joint, the inverse & forward dynamics was used on knee joint. A 6DOFs, deformable contact and ligaments were set on FT joint, which was same as normal knee joint. The 3 DOFs translation of FT joint was controlled by ligament force and FT surface deformable contact and solved through the quasi-static approach in Abaqus FEA implicit solver, while the rotation was controlled by the results of inverse kinematics. Ligaments were included to provide stability to the unconstrained joints in the TKR Knee model (Fig. 6). MCL was cut into 10 sections for generating the wrap constrain. The fraction between MCL and bone was also considered in model, where the fraction coefficient was set as 0.1. A hard contact was set on pressure-overclosure. What’s more, the muscle force should also be considered in the simulation. The force feedback was used in the model. With the muscles, ligaments and knee contact included, the dynamic equations of motion can be express as

$$\mathrm{M}\ddot{q} = r_{mus}F_{mus} + r_{lig}F_{lig} + r_{con}F_{con} + F_{ex} + G(q) + \mathrm{C}(q,\dot{q}) \tag{4}$$

where M is the mass matrix, $G(q)$ is a vector of forces arising from gravity, $C(q,\dot{q})$ are forces arising from the Coriolis and centripetal accelerations, and F_{ex} represents the generalized forces arising from external loads or prescribed accelerations. The force vectors arising from muscle (F_{mus}), ligament (F_{lig}), and contact force (F_{con}) are scaled by the moment arm matrices r_{mus}, r_{lig} and r_{con}, respectively.

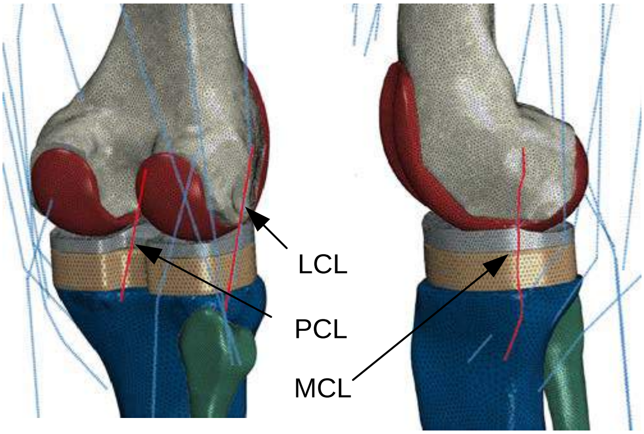

Figure.6. Ligaments around the knee joint

2.6 Model evaluation

The kinematic results are the fundamental data for the simulation. In this paper, a treadmill gait of fluoroscopy trial from the dataset was used to obtain an estimate of knee kinematics, namely flexion-extension rotation, internal-external rotation and abduction-adduction rotation. What's more, the subject-specific OpenSim Model, which was created based on JW's anatomic data from the dataset, was also used to estimate the kinematics results from simulation. The TF contact forces were estimated during a normal gait trial. Predictions were expressed as fractions of force and resampled on a gait cycle duration with a step interval of 0 from heel strike to the subsequent heel strike. The raw EMG measurements from 16 lower extremity muscles on the right leg during gait trial were used to verify the muscles' optimization results.

3. Results and discussion

The kinematic results extracted from the inverse kinematics which combine the shell element and distributed coupling feature from the motion data are shown in Figure 7. The method successfully tracks the measured knee flexion-extension (Fl-Ex), knee adduction-abduction (Ad-Ab) and knee internal-external (In-Ex) rotation with average root-mean-square errors (RMSE) of 4.4 degree, 2.9 degree and 2.3 degree respectively. The errors between simulation and measured results are mainly due to the difference between two test objects. The experimental results were measured by means of the treadmill instead of the true gait. What's more, the kinematics data of hip joint and ankle joint are not available on the dataset. The OpenSim model from dataset has been used on the kinematic verification, as also shown in Figure 7. A good agreement can be found from two simulation results. The RMSE of Fl-Ex, Ad-Ab and In-Ex rotation of knee joint and hip joint are 1.1 degree, 1.7 degree, 2.7 degree, 1 degree, 0.7 degree and 2.1 degree, respectively. All of the squared Pearson correlation coefficient (r^2) are larger than 0.95.

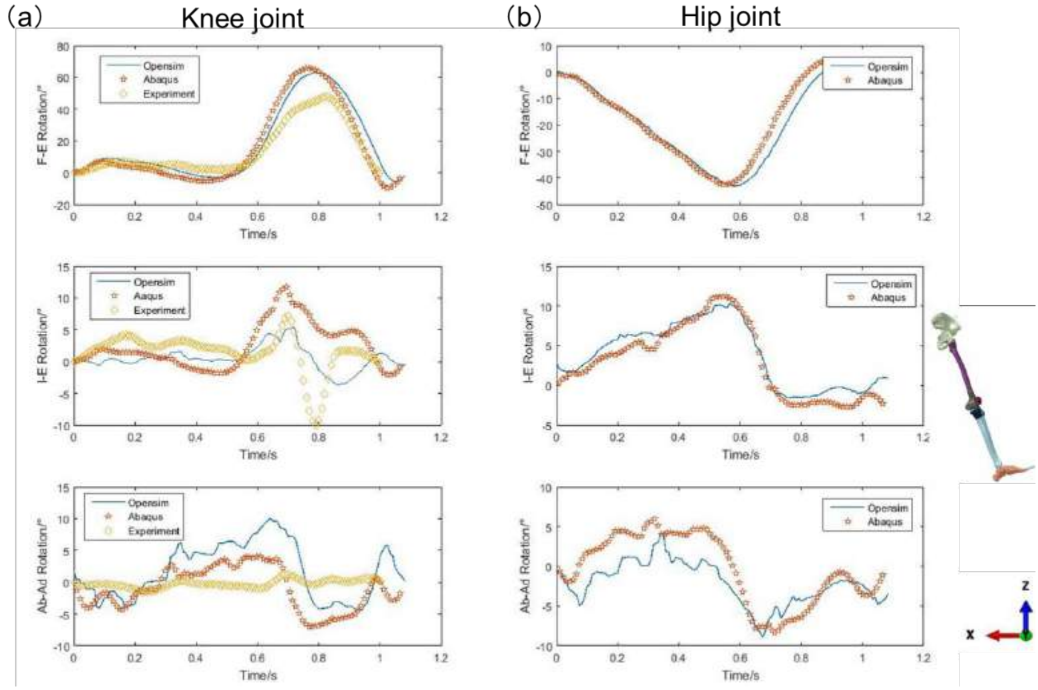

Figure.7. Kinematic verification for normal gait

Figure 8 provides the model predicted and measured knee joint loading for the normal gait trials. The temporal patterns of total TF contact forces are agreed well with the measurements, with an average temporal R^2 of 0.68, 0.87 and 0.75, respectively. The magnitude of estimates of anterior-posterior (AP) and medial-lateral (ML) contact forces were consistent well with that of measurements, with an RMSE error of 0.18 body weight (BW) and 0.05 BW. The axial force directly controls the magnitude of stress on prosthesis, which is an order of magnitude larger than the other two directions of the force. The predictions of the total TF contact forces exhibit the characteristic double peak in stance. The first and second total peak forces of 1.68 and 3.35 BW were 45% smaller and 37% greater than the experimental measurements of the corresponding peak force. Error in estimates of total axial contact force was slightly larger, with an average RMSE error of 0.63 BW (see Fig. 8(c)).

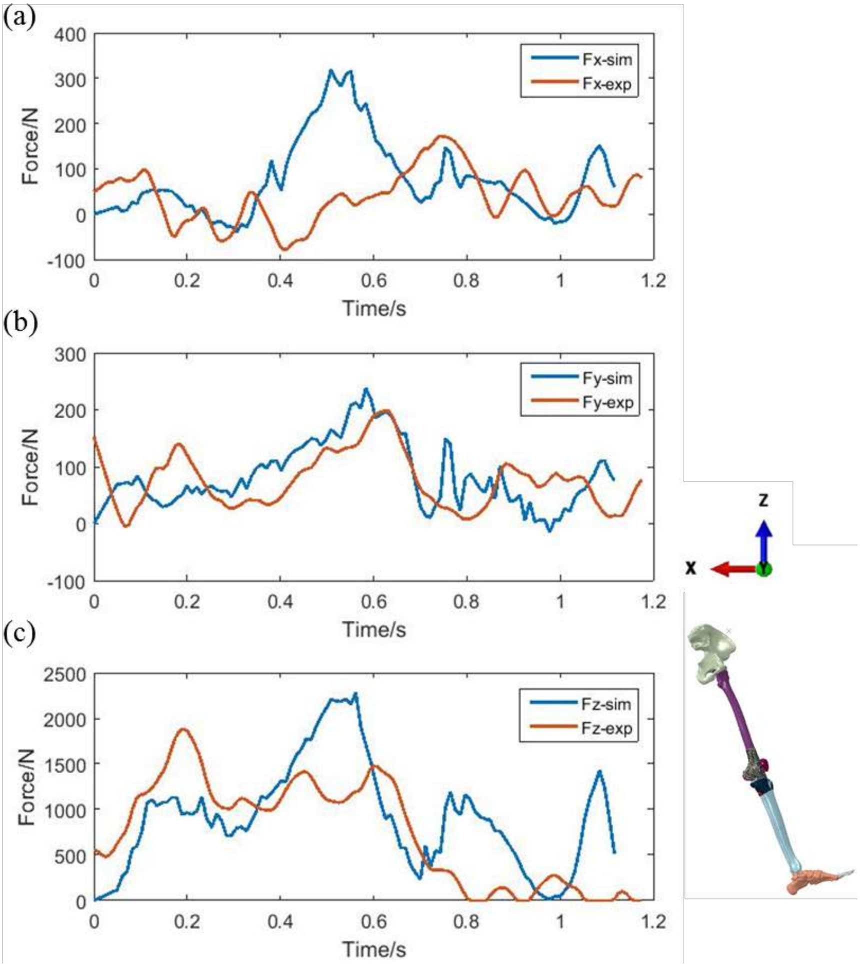

Figure.8. Experimental versus TF contact forces predicted during one gait trial (JW): (a) anterior-posterior force, (b) medial-lateral contact forces, (c) total axial contact force

A full normal gait ((jw_ngait_og1.c3d) from JW subject was applied to demonstrate how gait influences the Von Mises stress values and stress distribution on the prosthesis. Some of the important time nodes of gait are shown in Figure 9, which are heel strike (0%), foot flat (20%), heel rise (30%), terminal stance (40%), toe off (60%) and feet adjacent (80%). The simulation showed that the maximum Von Mises stress value of 94.9 MPa was achieved in the heel strike pose. The Von Mises stress in swing phase is much smaller than the stance phase.

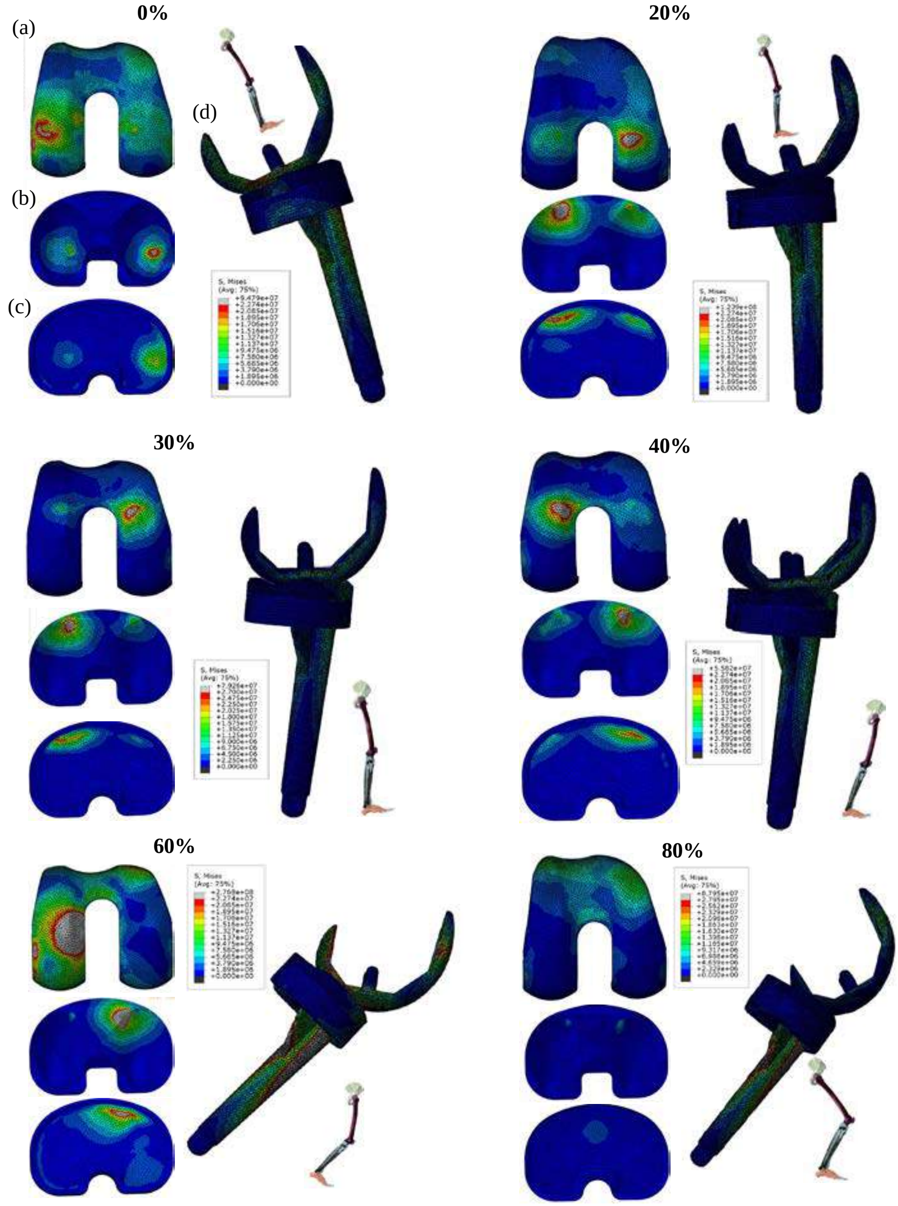

Figure.9. Misses stress distribution at different gait instants for contact surface of prosthesis (a) femoral component, (b) tibial insert component, (c) tibial tray component, (d) the TKR assembly.

4. Conclusion

We have introduced a framework based on concurrent dynamic finite element model (FEM) and patient-specific musculoskeletal (MS) technology for in vivo predicting the kinematics and contact mechanics within specific TKR knee joint and experimentally verified. The specified knee joint was interacted with muscle, ligament, and joint contact forces under the context of dynamic multi joint movement. It is initially shown that the concurrent framework can be used to predict knee stress distribution and knee joint force that compare well with those measured directly by an instrumented knee implant from the fourth and sixth “grand challenge competition to predict in vivo knee loads” database. There are still a number of limitations to be considered in our low limb model. We represented the ligaments as 1D axial elements, rather than deformable 3D representations that account for spatial variations in strain. In addition, there are large intra- and inter- subject variations for soft tissue properties, so the variability should also be considered. A user subroutine has been used on patella-femoral joint, which is controlled the movement of patella.

This study demonstrates the potential for co-simulating MS simulation and FEM under the context of coordinated multi-joint movement. The modeling framework has potential applications in aiding the subjective surgical planning in orthopedics procedures as a comprehensive tool for customer-made-prosthesis design.

5. Acknowledgment

The authors thank the knee load grand challenge team, led by B. J. Fregly, Ph.D. and Darryl D’Lima, M.D., Ph.D. (https://simtk.org/home/kneeloads), for providing the images, biomechanical measures, and in vivo knee contact forces used in this study. This research is supported by JSPS KAKENHI Grant Number 16H05874.

6. References

1. Marra, M. A，et.al, A Patient-Specific Musculoskeletal Model of Total Knee Arthroplasty to Predict In Vivo Knee Biomechanics. In: 5th Dutch Bio-Medical Engineering Conference 2015.
2. Marra, M. A，et.al, subject-specific musculoskeletal modeling framework to predict in vivo mechanics of total knee arthroplasty. Journal of biomechanical engineering, 2015, 137(2): 1-12.
3. Thelen, D. G, et.al, Co-simulation of neuromuscular dynamics and knee mechanics during human walking. Journal of biomechanical engineering, 2014, 136(2): 21-33.
4. Kalita, P., Schaefer, R. Mechanical models of artery walls. Archives of Computational Methods in Engineering, 2008, 15(1): 1-36.
5. Karjan, N. Multiphasic intervertebral disc mechanics: theory and application. Archives of Computational Methods in Engineering, 2012, 19(2): 261-339.

6. Quental, C., et al. Bone remodelling of the scapula after a total shoulder arthroplasty. Biomechanics and modeling in mechanobiology, 2014, 13(4): 827-838.
7. Completo, A., et al. Biomechanical evaluation of different reconstructive techniques of proximal tibia in revision total knee arthroplasty: An in-vitro and finite element analysis. Clinical Biomechanics, 2013, 28(3): 291-298.
8. Simon, U., et al. Influence of the stiffness of bone defect implants on the mechanical conditions at the interface—a finite element analysis with contact. Journal of biomechanics, 2003, 36(8): 1079-1086.
9. Sathasivam, S., et al. A computer model with surface friction for the prediction of total knee kinematics. Journal of Biomechanics, 1997, 30(2): 177-184.
10. Fregly, B. J., et al. Grand challenge competition to predict in vivo knee loads. Journal of Orthopaedic Research, 2012, 30(4): 503-513.
11. Lin, Y, et al. Simultaneous prediction of muscle and contact forces in the knee during gait. Journal of biomechanics, 2010, 43(5): 945-952.
12. Prabhav S, et. al, Results repeatability of right leg finite elements based musculoskeletal modeling, XXIV Congress of International Society of Biomechanics, 2013, 1-2.
13. Delp, S. L., et al. An interactive graphics-based model of the lower extremity to study orthopaedic surgical procedures. IEEE Transactions on Biomedical engineering, 1990, 37(8): 757-767.
14. Pioletti, D. P., et al. Viscoelastic constitutive law in large deformations: application to human knee ligaments and tendons. Journal of biomechanics, 1998, 31(8): 753-757.
15. Weiss, J. A.; et al. Ligament material behavior is nonlinear, viscoelastic and rate-independent under shear loading. Journal of biomechanics, 2002, 35(7): 943-950.
16. Quapp, K. M., Weiss, J. A. Material characterization of human medial collateral ligament. Journal of biomechanical engineering, 1998, 120(6), 757-763.
17. Eckhoff, D. G., et al. Three-dimensional mechanics, kinematics, and morphology of the knee viewed in virtual reality. J Bone Joint Surg Am, 2005, 87(2): 71-80.
18. Keerthi, S. S., et al. A fast iterative nearest point algorithm for support vector machine classifier design. IEEE transactions on neural networks, 2000, 11(1): 124-136.
19. Besl, P. J., McKay, N. D. Method for registration of 3-D shapes. International Society for Optics and Photonics, 1992, 586-606
20. Powers, C, M.. Patellar kinematics, part I: the influence of vastus muscle activity in subjects with and without patellofemoral pain. Physical therapy, 2000, 80(10): 956.